Available online at www.sciencedirect.com
ScienceDirect
ELSEVIER
Journal of Catalysis 243 (2006) 36–42
JOURNAL OF CATALYSIS
www.elsevier.com/locate/jcat

Shape selective and hydrogen spillover approach in the design of sulfur-tolerant hydrogenation catalysts

Hong Yang [a,*], Honglin Chen [a], Jinwen Chen [a], Oladipo Omotoso [b], Zbigniew Ring [a]

[a] *The National Centre for Upgrading Technology, Devon, AB T9G 1A8, Canada*
[b] *Advance Separation Technologies, 1 Oil Patch Drive, Devon, AB T9G 1A8, Canada*

Received 14 March 2006; revised 26 May 2006; accepted 24 June 2006

Abstract

This paper presents a novel approach to preparing sulfur-tolerant noble metal catalysts and the proof-of-concept experimental results. Our approach combines the concepts of shape selectivity and hydrogen spillover to the design of sulfur-tolerant catalysts. Platinum particles were encapsulated in the NaA-zeolite cages during zeolite synthesis. The pore opening was subsequently reduced by potassium ion exchange and chemical vapor deposition of tetraethyl orthosilicate (TEOS), allowing hydrogen molecules to enter but preventing hydrogen sulfide molecules from contacting the platinum particles. The success of platinum encapsulation in KA-zeolite was confirmed by XRD, H_2 and CO chemisorption, and TOF-SIMS techniques. A sulfur-tolerant catalyst was prepared by mixing TEOS-treated Pt/KA-zeolite with HY-zeolite and γ-alumina, and tested in the hydrogenation of naphthalene. Hydrogen species produced via dissociative adsorption of hydrogen molecules on platinum particles, situated inside KA-zeolite cages, migrated through surface diffusion to HY-zeolite and γ-alumina. Our experimental data demonstrated that the encapsulated platinum particles continuously generated hydrogen surface species that were used to hydrogenate naphthalene adsorbed on HY-zeolite and γ-alumina. These platinum particles showed resistance to sulfur poisoning when pure hydrogen was replaced by 3% H_2S in hydrogen in the naphthalene hydrogenation reaction.

Keywords: Platinum encapsulation; Shape selective; Hydrogen spillover; Naphthalene hydrogenation; Zeolite A; Chemical vapor deposition

1. Introduction

The gradual depletion of world oil reserves has led to the use of lower-grade, more aromatic feedstocks for motor fuel production. As required by currently adopted environmental- and performance-driven fuel specifications, the content of aromatics in diesel fuel is limited directly (Europe) or indirectly (U.S.). Commercially applied Co-Mo or Ni-Mo/Al_2O_3 hydrotreating catalysts have limited ability to hydrogenate these aromatics. Noble metal catalysts are highly active in aromatic hydrogenation; however, they are susceptible to sulfur poisoning even at concentrations of a few parts per million [1,2]. Therefore, these catalysts can be used only if the sulfur content in the feed has been reduced in a previous hydrotreating stage. For years, research groups from industry and academia have been working on the development of sulfur-tolerant noble metal catalysts. Several approaches have been taken to achieve this goal [3–9]. Acidic zeolite-supported platinum was reported to be more sulfur-resistant than alumina-supported platinum due to the stronger electron transfer to the acidic sites of the zeolite, which made platinum clusters more electron-deficient. This electron transfer, in turn, caused weaker sulfur-metal bonding and improved sulfur tolerance of the Pt/zeolite catalyst [3,4]. The sulfur tolerance of platinum clusters can be further improved by adding palladium as a promoter [6–8]. Lin et al. studied the aromatic hydrogenation over δ-Al_2O_3-supported Pt catalyst modified by adding a second metal, such as Co, Mo, Ni, Re, Ag, or Pd, in the presence of 1000 ppm sulfur from benzothiophene [6]. They found that Pd-Pt bimetallic catalyst was much more sulfur resistant than Pt catalyst. FFT-IR characterization of CO adsorbed on Pd, Pt, and Pd-Pt catalysts suggested that electrons were transferred from Pt to Pd by bimetallic interactions. The decreased electron density on Pt inhibited the H_2S

---

[*] Corresponding author.
E-mail address: hyang@nrcan.gc.ca (H. Yang).

0021-9517/$ – see front matter Crown Copyright © 2006 Published by Elsevier Inc. All rights reserved.
doi:10.1016/j.jcat.2006.06.026

adsorption, thereby enhancing sulfur tolerance. All of these approaches were aimed at increasing the electron deficiency of Pt via interaction with the support or a second metal. The major problem related to these approaches is that the noble metal particles are still accessible to sulfur-containing compounds, and poisoning through the formation of the sulfur-metal bond is inevitable.

Song [10] previously reported a different approach to designing noble metal catalysts for hydrotreating of sulfur-containing distillate. He proposed to use a zeolite support, mordenite, to prepare bimodal distributions of noble metal particles. Some metal sites are located in small pores with openings smaller than 5 Å, whereas others are contained in large pores with openings larger than 6 Å. The two pore systems interconnect or uniformly distribute so that the systems are close to each other. Diffusion of organosulfur compounds (such as thiophenic molecules) into small pores will be inhibited (shape selective exclusion). The large pores will allow fast diffusion and reaction of bulky polycyclic aromatics and sulfur molecules. Hydrogen molecules can readily enter both sizes of pores, dissociatively adsorb on metal particles, and be transported between pore systems by spillover. When the metal particles in large pores are deactivated by adsorbed sulfur molecules, spillover hydrogen from small pores can recover the poisoned metal sites. This approach is innovative, but neglects the presence of hydrogen sulfide, aliphatic sulfides (e.g., ethyl sulfide and propyl mercaptan), and small thiophenic molecules in the feed. Aliphatic sulfides are small enough to enter the 5-Å pores themselves. Furthermore, thiophenic sulfur compounds can be easily converted into H_2S under hydrotreating conditions, thereby causing deactivation of noble metal particles inside the small pores.

Linde type A zeolite has been used to encapsulate noble metal particles due to its small pore opening and low cost. NaA-zeolite has a pore opening of 4 Å, which can be modified to 5 or 3 Å by ion exchange with aqueous solutions of calcium or potassium salts [11]. A method for incorporating Pt particles into zeolite A was published in 1962 by Weisz et al. in the context of selective hydrogenation of linear olefins over branched olefins [12]. In 1993, this method was used by Ohgoshi et al. in the successful testing of hydrogenation of isobutylene by spillover hydrogen from Pt/KA-zeolite to NaY-zeolite [13]. None of these groups looked at the protection of Pt particles from sulfur poisoning. Interestingly, in 1966, a group of researchers from the French Petroleum Institute reported the use of Pt-promoted NaA-zeolite for the hydrogenation of ethylene in the presence of thiophene, dibenzothiophenes, and H_2S at about 60 °C [14]. They found that thiophene and dibenzothiophenes, being too large to enter the pores of the NaA-zeolite, did not inhibit the hydrogenation activity of ethylene; however, the catalytic activity completely disappeared in the presence of H_2S. This group reported no further efforts to reduce the pore size of Na-zeolite A to exclude H_2S.

Chemical vapor deposition (CVD) of silicon alkoxides has been used to modify the external surface properties and the pore openings of zeolites [15–17]. The CVD-modified zeolite catalysts have been used to selectively produce para-xylene in the alkylation of toluene [17]. ExxonMobil has patented a SiO_2-coated hydrogenation catalyst prepared by the reaction of silicon alkoxides with zeolite support to selectively hydrogenate ethylene over benzene [18]. CVD also has been used to narrow the pore opening of NaA-zeolite for various separation applications [19–21]. For example, Niwa et al. achieved selective separation of oxygen from nitrogen over NaA-zeolite modified by CVD of silicon methoxide [19]. Their work used the concept of shape selectivity only to achieve separation.

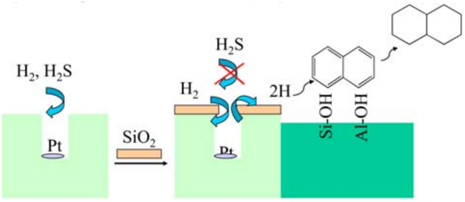

Fig. 1. Concept of sulfur tolerant noble metal hydrogenation catalyst.

In an attempt to design a family of sulfur-tolerant noble catalysts, we have developed a novel concept as elucidated schematically in Fig. 1. This concept is different from other approaches in that we aim to completely eliminate the contact between the sulfur-containing molecule and noble metal active sites. Our approach takes advantage of two mechanisms: shape selectivity and hydrogen spillover. First, the noble metal particles are incorporated into zeolite cages. The pore openings of the cages are sufficiently reduced to exclude hydrogen sulfide molecules (3.6 Å), the smallest sulfur-containing molecules in the hydrotreating process, while allowing hydrogen molecules (2.89 Å) and atomic hydrogen to diffuse in and out of the cage, respectively. Conceptually, the contact of sulfur molecules with noble metal particles can be completely eliminated in this manner. Meanwhile, the noble metal particles inside the zeolite pores are still accessible to hydrogen molecules, and the hydrogen species produced by the dissociation of hydrogen on the noble metal particles can spill over to the oxide support and hydrogenate the aromatic compounds adsorbed there. The concept of preventing contact between sulfur-containing compounds and noble metal active sites is intended to entirely eliminate the poisoning of the noble metals by sulfur compounds, thus enabling the use of these highly active noble metal catalysts for the hydrogenation of sulfur-containing feedstocks. To achieve this goal, platinum particles were incorporated into NaA-zeolite during synthesis. Pt/NaA-zeolite was then ion-exchanged with KCl solution to obtain Pt/KA-zeolite. The pore opening of Pt/KA-zeolite was further reduced by tetraethyl orthosilicate (CVD of TEOS).

2. Experimental

2.1. *Preparation of Pt/Na(K)A-zeolite*

Pt/NaA-zeolite was prepared according to the procedure of Weisz et al. [12]. Sodium aluminate ($Na_2O{\cdot}Al_2O_3{\cdot}3H_2O$, Anachemia) and sodium metasilicate (Na_2SiO_3, Aldrich) were used as aluminum and silicon sources, respectively. Three solutions were prepared for the synthesis: sodium aluminate in deionized water (solution A), sodium meta-silicate in deionized water (solution B), and $Pt(NH_3)_4Cl_2$ in deionized water (solution C). Solution A was first combined with solution C, to which solution B was added. The mixture was heated up to reflux and reacted under stirring for 7 h. The solid product was separated from the liquid phase by filtration and washed repeatedly with deionized water. The Pt/NaA-zeolite was ion-exchanged three times with 0.5 N KCl solution at 80 °C. The solid was thoroughly dried at room temperature, then dried at 120 °C for 2 h before calcination at 400 °C for 2 h. Pt/KA-zeolite was then subjected to two CVD cycles to further reduce the pore openings. In the CVD step, 2 g of catalyst was placed in the middle of a fixed-bed quartz reactor. Helium was flowed through a saturator filled with TEOS at 50 °C and then directed to the reactor. The CVD was conducted at 300 °C and followed by a calcination step at 400 °C to create new Si–OH sites for the next cycle. The TEOS-treated catalyst was denoted as TEOS_Pt/KA-zeolite. A blank KA-zeolite was synthesized the same way as Pt/KA-zeolite without the presence of the Pt precursor. For comparison of the platinum dispersion obtained by direct incorporation with that of ion exchange, platinum supported on a commercial NaA-zeolite (Aldrich) was prepared by ion exchange with an aqueous solution of $Pt(NH_3)_4Cl_2$ overnight at room temperature under stirring in an ultrasonic bath. The solid was dried at room temperature overnight and at 120 °C for 2 h, then calcined at 400 °C for 2 h. The Pt supported on commercial NaA-zeolite was denoted as Pt/NaA-com.

2.2. *Catalyst characterization*

The bulk elemental compositions (Pt, Al, Si, K, and Na) were measured by inductively coupled plasma-mass spectrometry (ICP-MS). The catalyst samples were first acid-digested under microwave heating. The detailed analytical procedure has been described elsewhere [22].

Platinum metal dispersion of the Pt/KA-zeolite was determined by H_2 chemisorption using a Micromeritics ASAP 2010C unit. The sample was degassed at 280 °C for 16 h. The reduction was carried out by flowing hydrogen at 110 °C for 0.5 h, at 200 °C for 0.5 h, and finally at 400 °C for 6 h (5 °C/min ramp rate). The system was evacuated at 35 °C for 60 min before an initial chemisorption analysis was performed at 35 °C to determine the total hydrogen uptake. The system was then evacuated for another 60 min at the same temperature to remove the physically adsorbed hydrogen. A repeat analysis was done at 35 °C after hydrogen was reintroduced. The difference between the initial and repeat analyses was used to calculate the metal dispersion. Preliminary screening of the sulfur resistance of the catalyst was carried out by first exposing the materials to 5% H_2S in hydrogen at 230 °C for 30 min, then readmitting the materials to hydrogen chemisorption. CO uptake of the catalyst was done in the same way as the H_2 chemisorption, but using CO as the probe molecule.

X-ray powder diffraction patterns of Pt/KA-zeolites were collected with a Rigaku DMAX-B rotating anode ($\mathrm{Co}K_\alpha$) diffractometer equipped with a curved graphite post sample monochromator. The diffractometer was scanned between 5° and 60° 2θ with a 0.02° step size. A divergent slit size of 0.167° and a receiving slit of 0.15 mm were used.

TOF-SIMS images were obtained using a TOF-SIMS IV instrument (ION-TOF GmbH). The catalyst pellet (Pt/KA-zeolite) was analyzed as prepared and after sputter etching for 1 h. A Ga gun with ion energy of 25 keV was used as a primary ion source for the analysis in a static (collimated) mode. An oxygen ion source (1 keV) was used for the sputter etching; the sputtered area was set at about 500×500 µm. Surface information of the top one or two atomic layers was obtained in both cases. A ca. 8×8 µm area was analyzed in the center of the etched area.

2.3. *Hydrogenation reaction*

Four catalysts were tested: (1) blank KA-zeolite (20 wt%) diluted with HY-zeolite (60 wt%) and γ-alumina (20 wt%); (2) Pt/KA-zeolite without dilution; (3) TEOS_Pt/KA-zeolite (20 wt%) diluted with HY-zeolite (60%) and γ-alumina (20%); and (4) Pt/KA-zeolite (20%) diluted with HY-zeolite (60%) and γ-alumina (20%). The fourth catalyst was used to investigate the effect of TEOS coating on hydrogenation activity. HY-zeolite (CVB720) was obtained from Zeolyst International (Valley Forge, PA). First, the powders of the catalyst components were physically mixed; then the mixture was pressed into pellets, which were crushed to 0.15–0.30 mm before being used as the final catalyst. In the hydrogenation test, 3 ml of catalyst was mixed with 3 ml of glass beads (0.25 mm) before being loaded into a fixed-bed microreactor (0.635×30.5 cm) operated in the continuous up-flow mode. The catalyst was reduced in situ at 400 °C overnight by a flow of hydrogen (350 ml/min) at 6.8 atm. Hydrogenation of naphthalene was carried out at 69 atm and 300 °C, with a liquid hourly space velocity (LHSV) of 2.0 h^{-1} and a hydrogen-to-liquid ratio of 1000 NL/L. Pure hydrogen was replaced by 3% H_2S in H_2 to test the sulfur resistance of the catalyst. Two back-to-back mass balance runs were conducted 24 h after the reaction conditions were reached. Details of the reactor system have been given elsewhere [23]. Naphthalene (5 wt%) in n-heptane was used as the feedstock. The feed and the products were analyzed using a HPLC device equipped with a Partisil 5 PAC column (Wharman) and a refractive index detector (Water) using 100% heptane as the mobile phase. Because only four general hydrocarbon groups—polyaromatics, di-aromatics, mono-aromatics, and saturates—could be identified by the HPLC method used, we simply followed the conversion of naphthalene and used its conversion as a measure of hydrogenation activity. Turnover frequency (TOF) was also calculated using first-order kinetics as an approximate measure for the hydrogenation reaction rate constant to compare the catalyst activity based on platinum.

3. Results and discussion

3.1. *Platinum encapsulation into zeolite cage*

The bulk compositions of Pt/KA-zeolite, TEOS_Pt/KA-zeolite, and Pt supported on commercial Na-zeolite (Pt/NaA-

Table 1
Elemental composition of catalysts and metal dispersions

	Catalyst ID		
	Pt/KA-zeolite	TEOS-Pt/KA-zeolite	Pt/NaA-com
Composition (wt%)			
Na	0.85	0.52	9.27
K	6.12	5.61	0.09
Al	8.39	7.90	8.42
Si	12.43	11.96	15.16
Pt	0.69	0.66	0.37
SiO_2/Al_2O_3	2.85	2.91	3.46
Lattice parameter a (Å)	24.5315	NA	24.5587
Dispersion (mol ratio)			
H/Pt	0.78	0.69	0.23
CO/Pt	0.36	0.03	NA

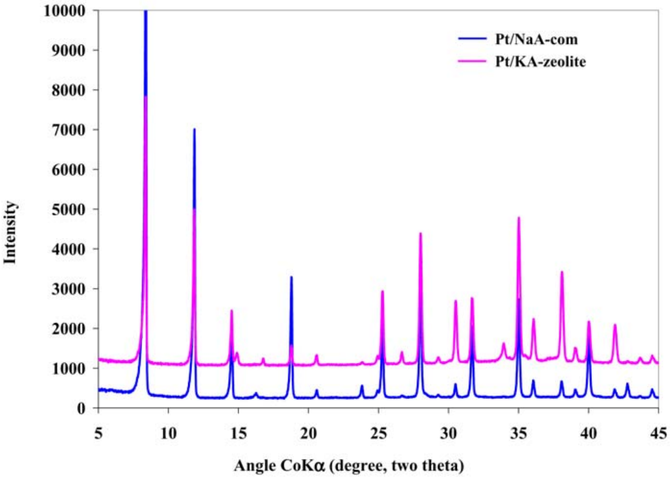

Fig. 2. XRD patterns of Pt/KA-zeolite and Pt/NaA-com.

com) were determined by ICP-MS. The results, along with the lattice parameters and metal dispersions for these catalysts, are presented in Table 1. The results show that the synthesized Pt/KA-zeolite has a SiO_2/Al_2O_3 molar ratio of 2.85, similar to that of the commercial NaA-zeolite, and is in the range of the synthetic zeolite A [11]. The TEOS_Pt/KA-zeolite has a slightly higher SiO_2/Al_2O_3 molar ratio (2.91) due to the CVD deposition of silica.

The XRD patterns of Pt/KA-zeolite and Pt/NaA-com are compared in Fig. 2. Pt/KA-zeolite is essentially crystalline of the K-exchanged zeolite A, with minor amounts of K-natrolite impurity and an amorphous component. Pt/NaA-com also contains minor amounts of sodalite impurity and an amorphous component. A LeBail fit of the diffraction patterns shows that the K-exchanged form has a smaller lattice parameter than the Na form (Table 1). The high crystallinity of Pt/KA-zeolite shows that incorporating 0.69 wt% of platinum into zeolite synthesis mixture has a minimal impact on the crystal structure of zeolite A.

A high Pt dispersion of 0.78 (H/Pt) was obtained by directly incorporating platinum into the zeolite initial synthesis mixture (Table 1). The ion-exchanged commercial Pt/NaA-com had a much lower platinum dispersion, as expected, due to the relative size of $[Pt(NH_3)_4]^{2+}$ ions compared with the zeolite pore opening. A similar trend was also observed by other groups for Pt- and Rh-exchanged A-zeolite [24–26]. The size of the platinum particles for the Pt/KA-zeolites was estimated as 13.8–14.5 Å from the dispersion data assuming spherical particles [27], close to the dimension of the (11.4 Å) α cage in zeolite A [11]. Zeolite A has two types of cages: α cage and ß (or sodalite) cage. The aperture of the α cage is an eight-member ring with a diameter of 4.1 Å for NaA-zeolite and 3.0 Å for KA-zeolite; the aperture of the ß cage is a six-member ring with a diameter of 2.2 Å. Platinum can be incorporated into both types of cages when platinum precursors are initially present in the synthesis mixture. Although the hydrogen molecule can easily penetrate the opening of the α cage under the chemisorption conditions (35 °C and 1 atm), a higher temperature is required for the hydrogen molecule to overcome the energy barriers to enter the sodalite cage [28,29]. In other words, the platinum particle's size estimated by hydrogen chemisorption might be larger than the actual size. Nevertheless, the platinum particle size estimated by chemisorption indicated that platinum particles were confined in the zeolite cages and that no migration to the external surface occurred during preparation.

The hydrogen chemisorption result was supported by the TOF-SIMS observations. Two sets of TOF-SIMS images were collected to determine the distribution of platinum in the prepared Pt/KA-zeolite catalyst. The first of these was for the untreated catalyst pellet, which gave information of the top one or two atomic layers of as-prepared samples; the second was taken after removal of the top layers by 1 h of sputtering. The depth of the sputtering was not determined because of the lack of standards and the porous nature of the zeolite. Figs. 3a and 3b illustrate the TOF-SIMS images for Pt/KA-zeolite. As illustrated in Fig. 3a, there was barely any platinum detected in the untreated samples, indicating that no platinum was deposited on the external surface or within the top few monolayers. After 1 h of etching, however, platinum was well exposed and homogeneously distributed in the sample (Fig. 3b).

Our results closely agree with the results published by other groups [12,25,26,30]. Rossin and Davis prepared rhodium zeolites as catalysts for the hydroformulation of alkenes in the gas and liquid phases [30]. They used several methods, including ion exchange of NaA-zeolite with aqueous solution of $RhCl_3$, adding RhNaA-zeolite as a seed in the NaA-zeolite synthesis gel, and adding $RhCl_3 \cdot xH_2O$ directly to the synthesis gel to incorporate rhodium into NaA-zeolite. The RhNaA-zeolite was then converted to RhCaA-zeolite by ion exchange with $CaCl_2$ at room temperature. Rossin and Davis evaluated the surface-to-bulk rhodium content by comparing the rhodium content obtained from X-ray photoelectron spectroscopy (XPS) with that of bulk chemical analysis (CA). They found that rhodium was incorporated into RhCaA zeolite by all methods (XPS/CA: 1–5) except ion exchange, where rhodium was located mainly on the external surface (XPS/CA: 60).

For NaA-zeolite, when the sodium ion is replaced by a divalent cation such as calcium, the pore aperture will increase from 4 to 5 Å due to the absence of ions at site II of the eight-member rings. However, when the sodium ion is exchanged with a larger univalent cation, such as potassium, the pore aper-

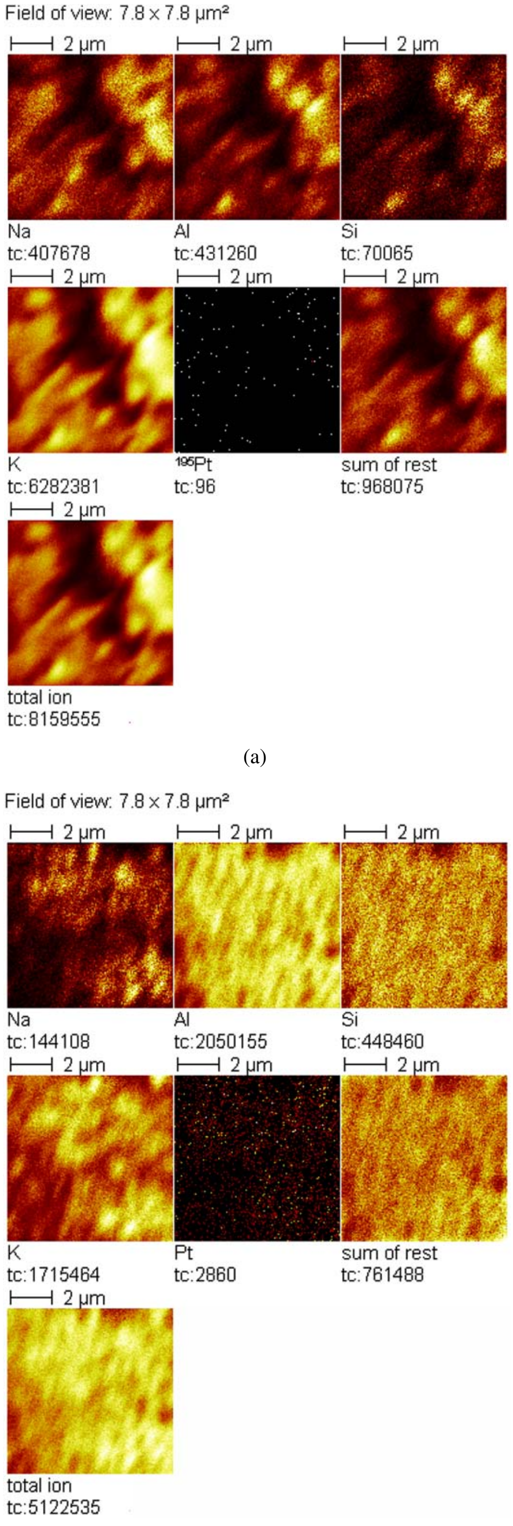

(a)

(b)

Fig. 3. (a) Initial TOF-SIMS image of Pt/KA-zeolite, (b) TOF image of Pt/KA-zeolite after 1 h etching.

ture decreases to 3 Å, because potassium ions in site II restrict free access to the eight-member rings and prevent molecules larger than 3 Å from entering the supercage [11]. This phenomenon was observed by Ohgoshi et al. [13] in Pt/KA-zeolite, where dispersion values of 0.83 and 0.01 were obtained for H/Pt and CO/Pt, respectively, by measuring hydrogen and carbon monoxide chemisorption. This suggests that the pore size of the potassium-exchanged zeolite was small enough to prevent the CO molecule (3.76 Å) from entering. In this work, a CO/Pt value of 0.36 (Table 1) was obtained for Pt/KA-zeolite, indicating that CO was not completely excluded from entering the pore after Na ions were replaced by K ions through ion exchange.

Several facts should be considered when explaining the observed accessibility of the platinum sites to CO molecules. First, regarding the degree of ion exchange, in our Pt/KA-zeolite, the sodium content was 0.85 wt%, whereas it was <0.1 wt% in Ohgoshi's study. Second, incorporation of platinum inside the supercage may shift the potassium ion away from the ideal site II, reducing its restricting effect on the pore opening. Third, platinum(II) might have some effect on the pore aperture, as is the case for other divalent ions such as calcium (e.g., increasing pore openings). The coexistence of platinum and potassium would result in an A-zeolite with a pore opening larger than that of potassium-exchanged zeolite A.

To entirely block access of the CO molecule to the platinum particles, the pore opening of Pt/KA-zeolite was further reduced by CVD of TEOS. The TEOS_Pt/KA-zeolite had a CO/Pt value of 0.03, significantly lower than that of Pt/KA-zeolite (0.36). In contrast, the hydrogen uptake decreased slightly for the TEOS_Pt/KA-zeolite (H/Pt value of 0.69) compared with that of the Pt/KA-zeolite (H/Pt value of 0.78). The results indicate that CVD is an effective method for tailoring the pore openings of zeolite. CO (3.76 Å) was successfully prohibited while H_2 still enjoyed free access to the platinum inside of the zeolite cage.

3.2. *Preliminary test for sulfur resistance*

A preliminary test was set up at our center to screen the catalyst materials for sulfur resistance. Catalysts that showed promising results were further tested for hydrogenation activity in the fixed-bed reactor. In this case, the catalyst was submitted to an initial hydrogen chemisorption analysis, then a second hydrogen chemisorption analysis after being exposed to 5% H_2S in hydrogen for 30 min at 230 °C. Fig. 4 compares the H_2 uptakes for TEOS_Pt/KA-zeolite and Pt/KA-zeolite before and after H_2S poisoning. After exposure to H_2S, the TEOS_Pt/KA-

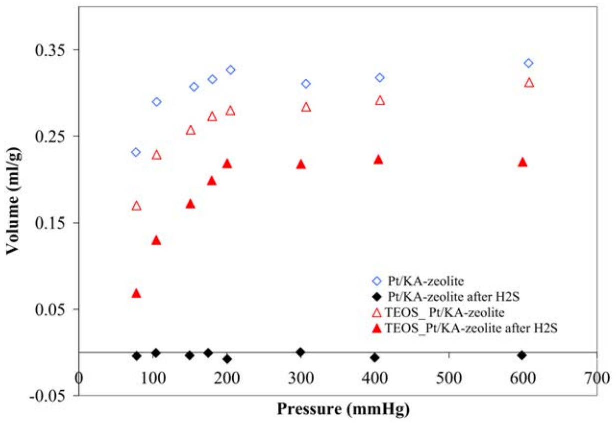

Fig. 4. Comparison of hydrogen uptake before and after H_2S poisoning.

zeolite retained >60% of its original hydrogen adsorption capacity, whereas a complete loss of hydrogen adsorption capacity was observed for the Pt/KA-zeolite not treated with TEOS. These results, combined with those of CO chemisorption, suggest that although CO (3.76 Å) was partially excluded from entering the pores of Pt/KA-zeolite, H_2S (3.6 Å) was still sufficiently small to reach the platinum particles inside the zeolite cage. The pore opening was further reduced through TEOS treatment; in TEOS_Pt/KA-zeolite, our results reveal at least 60% of platinum particles located in the zeolite pores were smaller than H_2S but larger than H_2. The rest of the platinum particles were probably found inside the pores with diameters >3.6 Å, due to insufficient TEOS treatment. Our experiment successfully demonstrated that platinum particles inside zeolite pores were protected from exposure to H_2S due to a shape-selective effect.

3.3. Hydrogenation of naphthalene

The hydrogenation activity tests of the catalysts were conducted in a small fixed-bed continuous reactor at 300 °C, 69 atm of hydrogen pressure, and a LHSV of 2.0 h^{-1}. Naphthalene (5 wt%) in *n*-heptane was used as the feed. Two back-to-back runs were conducted at each condition when the reactions reached steady state, as determined by measuring the density of the liquid product (which took 20–22 h). Averaged results from the two runs were used. The conversion of naphthalene was followed by HPLC. The turnover frequency was calculated assuming first-order kinetics for the hydrogenation reaction.

Table 2 presents the compositions of catalyst mixtures, the conversions of naphthalene, and the TOFs of corresponding catalysts. When pure hydrogen was used as the treatment gas, naphthalene conversion over the blank catalyst (without Pt)—a mixture of KA-zeolite, HY-zeolite, and γ-alumina—was 0.85%. A comparable conversion of 1% (TOF = 0.3) was obtained over Pt/KA-zeolite with no diluent added. Because naphthalene is too bulky for the pore openings of KA-zeolite and can be converted only over the support and the surface platinum particles, we can assume that the 1% conversion was caused by the support and that practically all platinum particles were located inside the zeolite pores. In the case of the hybrid catalyst—a mixture of TEOS_Pt/KA, HY-zeolite, and γ-alumina—naphthalene conversion of 9.7% (TOF = 6.3) was reached. When pure hydrogen was replaced by 3% H_2S in hydrogen, the hybrid catalyst system retained 38% of its original hydrogenation activity based on the amount of active metal, indicating that our newly designed catalyst is highly sulfur-tolerant. Although the mechanism of sulfur resistance in our case differs from other published approaches, it is still interesting to compare our results with previously reported data. Song and Schmitz investigated the hydrogenation of naphthalene over zeolite-supported palladium and platinum catalysts [4]; at 200 °C and 68 atm, complete conversion of naphthalene was obtained over 2 wt% Pd/mordenite and 2 wt% Pt/mordenite. With Pd/mordenite catalysts, the conversion decreased to 40.3% in the presence of 1098 ppm sulfur from benzothiophene and it decreased to 2.9% in the presence of 895 ppm sulfur for Pt/mordenite. Lin et al. studied the hydrogenation of tetralin over δ-Al_2O_3-supported Pt catalysts modified by adding a second metal [6]. Pd-Pt was the best combination for sulfur tolerance. At 280 °C and 26 atm, the conversion of tetralin under 1000 ppm sulfur from benzothiophene was 7.1% after 4 h on stream, a decrease from the initial conversion of 73.3%.

Table 2
Comparison of naphthalene hydrogenation activity (69 atm, 300 °C, LHSV 2.0)

Catalyst mixtures	Conversion naphthalene (%)	TOF (s^{-1} Pt^{-1})
KA-zeolite + HY-zeolite + γ-alumina	0.85	NA
Pt/KA-zeolite	1	0.3
TEOS_Pt/KA-zeolite + HY-zeolite + γ-alumina	9.7	6.3
Switch from pure hydrogen to 3% H_2S	3.9	2.4
Pt/KA-zeolite + HY-zeolite + γ-alumina	15.27	10.3

As mentioned above, H_2 chemisorption shows that 60% of the initial hydrogen uptake was preserved after H_2S poisoning. The discrepancy between the sulfur resistance of platinum in H_2 chemisorption and the pilot plant test is probably due to the difference of the two systems. Chemisorption was conduced at 35 °C and low H_2 pressure, whereas the pilot plant test was conducted at high H_2 pressure and 300 °C and in the presence of naphthalene and heptane. The last row in Table 2 shows that the Pt/KA-zeolite has significantly higher hydrogenation activity than that of TEOS-treated Pt/KA-zeolite, which shows a loss of catalyst activity due to silica deposition. A similar trend was observed by Degnan and Johnson in a U.S. patent [17]. These authors coated Pt/ZSM-$5SiO_2$ catalyst with silica to promote the hydrogenation selectivity of ethylene over benzene. After two cycles of silica impregnation, they observed a 2.7-fold decrease in benzene hydrogenation activity and a 1.9-fold decrease in ethylene hydrogenation activity.

Hydrogen spillover refers to surface diffusion of hydrogen surface species from the metal sites where they are produced by the dissociation of hydrogen molecules to the oxide support that has no activity for dissociative hydrogen adsorption [31]. The hydrogen species could be consumed in a hydrogenation reaction over the oxide support. Although the phenomenon of hydrogen spillover is commonly accepted, there still exists some ambiguity as to whether or not the spillover hydrogen species can produce substantial catalytic effects on the support and enhance chemical reactions [13,32–36]. Cęckiewicz and Delmon found that the hydrogenation activity of benzene increased about 4-fold when 0.6 wt% Pt/γ-alumina was diluted with alumina at a ratio of 1:20. Their results suggest that benzene hydrogenation occurred on both Pt/γ-alumina and alumina due to a hydrogen spillover effect [32]. On the other hand, Miller and Pei studied the hydrogenation reaction of ethylbenzene over a mixture of Pt/Na-zeolite and H-USY-zeolite preadsorbed with ethylbenzene in the presence of D_2 at 75 °C, and found that the reaction of ethylbenzene with spillover deuterium resulted in isotopic exchange, but not in saturation of aromatic rings [35]. To the best of our knowledge, there have been no published results concerning the hydrogenation of diaromatics such as naphthalene with spillover hydrogen. The present work has clearly demonstrated the significant contribution of hydrogen spillover to hydrogenation of naphthalene for the first time. Hydrogen is dissociated on the Pt particles within the pores of Pt/KA-zeolite, and the spillover hydrogen migrates to the surrounding HY-zeolite and γ-alumina, where naphthalene molecules are adsorbed and hydrogenated.

4. Conclusion

Our experimental results demonstrate that it is possible to design a new family of sulfur-resistant catalysts by combining the concepts of shape selectivity and hydrogen spillover. These novel materials could possibly find applications as a catalyst component for hydrogenation/dehydrogenation, isomerization, reforming, and oxidation processes, enhancing the overall rate by supplying spillover hydrogen. They also can be used in membrane manufacturing to increase the permeability and permselectivity of hydrogen in the separation of gas mixtures, or as membrane reactors for dehydrogenation and reforming. Future work is planned at NCUT to improve hydrogenation activity and evaluate the resistance to ammonia and organic nitrogen compounds.

Acknowledgments

Partial funding for this work was provided by the Canadian Program for Energy Research and Development (PERD), the Alberta Research Council, and The Alberta Energy Research Institute. The authors thank Drs. Dimitre Karapuzov and Anqiang He of ACSES for the TOF-SIMS analysis, the NCUT staff for the hydrogenation reaction analyses, and Norman Sacuta for editorial assistance.

References

[1] C.H. Bartolomew, P.K. Agarwal, J.R. Katzer, Adv. Catal. 31 (1982) 135.

[2] J. Barbier, E. Lamy-Pitara, P. Marecot, J.P. Boitiaux, J. Cosyns, F. Verna, Adv. Catal. 37 (1990) 279.

[3] R.A. Dalla Betta, M. Boudart, in: L.V. Rees (Ed.), Proceeding of the Fifth International Congress on Catalysis, Miami Beach, FL, 1972, p. 1329.

[4] C.S. Song, A.D. Schmitz, Energy Fuels 11 (1997) 656.

[5] Y. Yoshimura, H. Yasuda, T. Sato, N. Kijima, T. Kameoka, Appl. Catal. A 207 (2001) 303.

[6] T.B. Lin, C.A. Jan, J.R. Chang, Ind. Eng. Chem. Res. 34 (1995) 4284.

[7] T. Fujikawa, K. Idei, K. Ohki, H. Mizuguchi, K. Usui, Appl. Catal. A 205 (2001) 71.

[8] H. Yasuda, Y. Yoshimura, Catal. Lett. 46 (1997) 43.

[9] B. Delmon, G. Froment, Catal. Rev. Sci. Eng. 38 (1996) 69.

[10] C.S. Song, CHEMTECH 29 (1999) 26.

[11] D.W. Breck, Zeolite Molecular Sieve, Structure, Chemistry, and Use, Wiley, New York, 1974.

[12] P.B. Weisz, V.J. Frilette, R.W. Maatman, E.B. Mower, J. Catal. 1 (1962) 307.

[13] S. Ohgoshi, I. Nakamura, Y. Wakushima, Stud. Surf. Sci. Catal. 77 (1993) 289.

[14] B. Juguin, C. Clement, P. Leprince, R. Montaranl, Bull. Soc. Chim. France 7 (1966) 709.

[15] M. Niwa, S. Kato, T. Hattori, Y. Murakami, J. Chem. Faraday Trans. I 80 (1984) 3135.

[16] C.T. O'Connor, K. Möller, H.J. Manstein, J. Mol. Catal. A 181 (2002) 15.

[17] J.H. Kim, A. Ishida, M. Okajima, M. Niwa, J. Catal. 161 (1996) 387.

[18] T.F. Degnan, I.D. Jonhson, U.S. patent 2002107139 A1, 2002.

[19] M. Niwa, K. Yamazaki, Y. Murakami, Ind. Eng. Chem. Res. 30 (1991) 38.

[20] M. Niwa, Y. Yamazaki, Y. Murakami, Ind. Eng. Chem. Res. 33 (1994) 371.

[21] C.D. Chudasama, J. Sebastian, R. Jasra, Ind. Eng. Chem. Res. 44 (2005) 1780.

[22] S.L. Wu, Y.H. Zhao, X.B. Feng, A. Wittmeier, J. Anal. Atm. Spectrom. 11 (1996) 287.

[23] H. Yang, M. Wilson, C. Fairbridge, Z. Ring, Energy Fuels 16 (2002) 855.

[24] R.D. Shannon, J.C. Vedrine, C. Naccache, F.J. Lefebvre, J. Catal. 88 (1984) 431.

[25] M.E. Davis, C. Saldarriaga, J.A. Rossin, J. Catal. 103 (1987) 520.

[26] R. Vijaylakshmi, S. Kapoor, S.K. Kulshreshtha, Solid State Sci. 4 (2002) 489.

[27] J.L. Lemaiter, P.G. Menon, F. Delannay, in: F. Delanny (Ed.), Characterization of Heterogeneous Catalysts, Dekker, New York, 1984, p. 340.

[28] J. Weitkamp, M. Fritz, S. Ernst, Int. J. Hydrogen Energy 20 (1995) 967.

[29] A.M. Efstathiou, E.V.R. Borgstedt, S.L. Suib, C.O. Bennett, J. Catal. 135 (1992) 135.

[30] J.A. Rossin, M.E. Davis, J. Chem. Soc. Chem. Commun. (1986) 234.

[31] W.C. Conner, J.L. Falconer, Chem. Rev. 95 (1995) 759.

[32] S. Cęckiewicz, B. Delmon, J. Catal. 108 (1987) 294.

[33] J. Wang, L. Huang, Q. Li, Appl. Catal. A (1998) 191.

[34] J.T. Miller, S. Pei, Appl. Catal. A 168 (1988) 1.

[35] N.I. Najafabadi, G. Chattopadhyaya, K.J. Smith, Appl. Catal. A 235 (2002) 47.

[36] P.A. Sermon, G.C. Bond, Catal. Rev. 8 (2) (1973) 211.